



Self-Immolative Polymers with Potent and Selective Antibacterial Activity by Hydrophilic Side Chain Grafting

| | |
|-------------------------------|--|
| Journal: | <i>Journal of Materials Chemistry B</i> |
| Manuscript ID | TB-ART-06-2018-001632.R2 |
| Article Type: | Paper |
| Date Submitted by the Author: | 11-Jul-2018 |
| Complete List of Authors: | Palermo, Edmund; Rensselaer Polytechnic Institute, Materials Sci and Eng Ergene, Cansu; Rensselaer Polytechnic Institute, Materials Sci and Eng |
| | |

SCHOLARONE™
Manuscripts

Self-Immolative Polymers with Potent and Selective Antibacterial Activity by Hydrophilic Side Chain Grafting

Cansu Ergene and Edmund F. Palermo*

*Department of Materials Science and Engineering, Rensselaer Polytechnic Institute,
110 8th St., Troy, New York 12180, USA*

*Email: palere@rpi.edu

Abstract. We report the first example of a self-immolative polymer that exerts potent antibacterial activity combined with relatively low hemolytic toxicity. Specifically, self-immolative poly(benzyl ether)s bearing pendant cationic ammonium groups and grafted poly(ethylene glycol) chains in the side chains were prepared via post-polymerization thiol-ene chemistry. These functional polymers undergo sensitive and specific triggered depolymerization into small molecules upon exposure to a designed stimulus (in this example, fluoride ion cleaves a silyl ether end cap). The molar composition of the resulting statistical copolymers was varied from 0 to 100% PEG side chains. The average molar mass of the pendant PEG chains was either 800 or 2000 g/mol. The antibacterial and hemolytic activities were evaluated as function of copolymer composition. Strong bactericidal activity (low $\mu\text{g/mL}$ MBC) was retained in copolymers containing 25 – 50% PEG-800, whereas hemolytic toxicity monotonically decreased (up to $\text{HC}_{50} > 1000 \mu\text{g/mL}$) with increasing PEG content. PEG-2000 was far less effective; both the MBC and HC_{50} decreased to a comparable extent with increasing PEGylation. Overall, the best cell type selectivity index ($\text{HC}_{50}/\text{MBC} \sim 28$) was obtained for the copolymer containing ~ 50% cysteamine and ~50% PEG-800 side chains, as compared to the cationic homopolymer ($\text{HC}_{50}/\text{MBC} < 1$). Thus, systematic tuning of PEG graft density and chain length effectively enhances the cell-type selectivity of these self-immolative polymers by orders of magnitude.

1 Introduction

2
3 The alarmingly rapid proliferation of antibiotic-resistance bacterial infections, compounded
4 by the continuously declining number of new antibiotic drug approvals, is a global health crisis.
5 The urgency of this problem has led many researchers to seek new antibacterial agents¹⁻³. Host
6 defense peptides (HDPs) are components of innate immunity that exert antibacterial efficacy
7 with minimal toxicity to host cells⁴⁻⁶. Synthetic mimics of HDPs including β -peptides⁷,
8 peptoids⁸, nylon-3 copolymers⁹, polymethacrylates¹⁰⁻¹², polymethacrylamides,¹³
9 polycarbonates¹⁴⁻¹⁷ and polynorbornenes¹⁸⁻²⁰, are designed to capture the essential
10 physiochemical features of the peptides: cationic charge, hydrophobicity, and short chain
11 length.²¹⁻²⁵ HDPs and their synthetic mimics are widely thought to exert a mechanism of action
12 involving membrane disruption^{26, 27} and are less likely to induce bacterial resistance as compared
13 to conventional antibiotic drugs²⁸. Still, HDPs are expensive to manufacture and are rapidly
14 degraded by proteases *in vivo*²⁹, which motivates the continued development of biomimetic
15 synthetic polymers.³⁰⁻³²

16 In contrast to the proteolytic instability of HDPs, vinyl-based synthetic antibacterial polymers
17 do not degrade appreciably in physiological conditions. Their chemical stability may restrict
18 biomedical use due to long-term toxicity *in vivo*, even if they are non-toxic in short-term *in vitro*
19 studies^{17, 33}. Thus, biodegradable antibacterial polymers such as polyesters^{33, 34}, polycarbonates^{15,}
20 ³⁵ and even acetal networks³⁶ are of increasingly high interest. These polymers are subject to
21 cleavage at random sites along the backbone of the polymer chains, thus representing a passive
22 degradation rate that is dictated by the chemical structure of the linkage and the solvent-
23 accessibility of the microenvironment³⁷. In contrast to conventional biodegradable polymers,
24 metastable “self-immolative” polymers (SIMPs) undergo triggered end-to-end depolymerization

1 in response to a specific stimulus.³⁸ Upon the cleavage of a labile ω -end-cap, above the ceiling
2 temperature T_c , the active species of depropagation is liberated and the chain will spontaneously
3 unzip into its component monomers.³⁹⁻⁴² This unique phenomenon provides marked signal
4 amplification, as well as mechanical transduction of chemical signals, and the unparalleled
5 specificity to control the onset of chemical degradation (rather than simply tuning the passive
6 release profile). SIMPs have been used in applications of drug delivery⁴³⁻⁴⁵, biosensors⁴⁶,
7 microfluidics⁴⁷ and dynamically recyclable plastics^{48, 49} but were not utilized in antimicrobial
8 platforms until very recently. In the context of antibacterial materials development, self-
9 immolation provides a unique opportunity to trigger the conversion from polymer to small
10 molecule, which dramatically alters the mechanical properties and solubility characteristics of
11 the material, on demand. One may envision application in “smart” bio-responsive coatings that
12 mediate triggered release of biologically active small molecules into the surrounding media.

13 We recently reported the first example of a biocidal self-immolative polymer⁵⁰ based on
14 modifications to the poly(benzyl ether) (PBE) platform pioneered by Phillips and co-workers.^{51, 52}
15 The cationic PBEs bearing primary amine groups displayed rapid, broad-spectrum antibacterial
16 activity and were readily depolymerized into small molecules upon introduction of chemical
17 “trigger”. However, these first-generation cationic PBEs are also highly toxic to red blood cells
18 (RBCs). We hypothesized that the intensely hydrophobic nature of the PBE backbone leads to
19 the high hemolytic toxicity and limits aqueous solubility. In this work, we present a simple
20 PEGylation strategy to decrease the overall hydrophobicity of the PBEs and thus reduce the
21 hemolytic toxicity, while retaining the antibacterial potency.

22 The classical approach to HDP-mimetic design involves optimization of two key features in a
23 polymer structure: the cationic charge and the hydrophobicity. However, binary copolymers

1 were found to contain both higher cationic charge density and higher hydrophobicity than the
2 average HDP.⁵³ It is clear that HDPs are not solely composed of cationic and hydrophobic
3 residues, but also contain an abundance of neutral, hydrophilic groups. Consequently, ternary
4 copolymer systems containing neutral, hydrophilic groups (hydroxyls,^{54, 55} sugars,^{56, 57}
5 Zwitterions,⁵⁸ PEG^{59, 60}) have been studied. Incorporation of the third component played an
6 important role in modulating the cell-type selectivity of a polymer by reducing the hemolytic
7 toxicity while maintaining (or even improving) the antibacterial efficacy. Youngblood and co-
8 workers reported⁶¹ ternary antimicrobial copolymers of hydrophobically quaternized 4-vinyl
9 pyridine (4VP) with PEG methacrylate. Compared to highly antibacterial and hemolytic
10 quaternized PVP, the PEGylated copolymers exhibited lower hemolytic toxicity and their
11 retained antibacterial activity.⁶¹

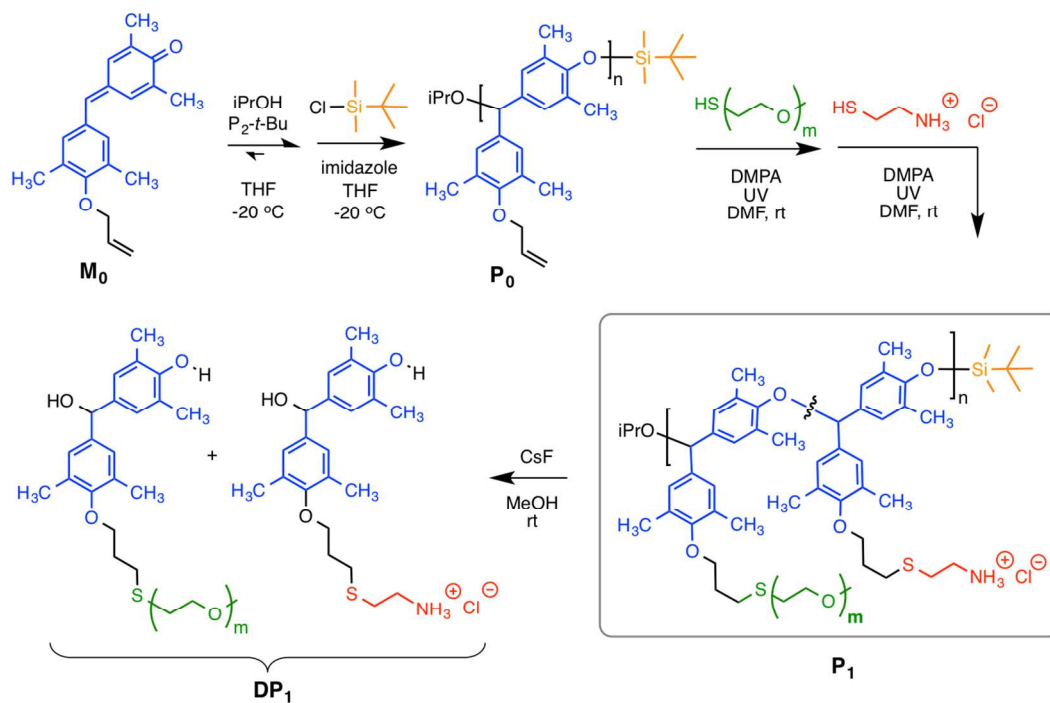
12 In this paper, we modified cationic PBEs with varying content of PEG grafts in the side
13 chains to quantify the effects of reducing hydrophobicity on the antibacterial and hemolytic
14 activities. Poly (benzyl ether)s with allyl side chains and silyl ether end-caps were synthesized
15 based on modifications to the route recently described by Phillips and co-workers⁵¹. Relative to
16 the first-generation cationic PBEs, the PEGylated variants exhibited lower hemolytic toxicity
17 while maintaining comparable level of antibacterial potency. The best example showed a 28-fold
18 selectivity toward *E. coli* over red blood cells, which is a remarkable improvement over our first-
19 generation biocidal SIMPs, which gave a selectivity index of < 1 .

20

21 **Results and Discussion**

22 **Polymer Synthesis.** We prepared a library of PBEs with PEGylated and cationic side chains,
23 in various copolymer ratios and with two different PEG chain lengths (Figure 1). Briefly, anionic

1 polymerization was carried out at $-20\text{ }^{\circ}\text{C}$ in THF, which is below the ceiling temperature of PBE
 2 ($T_c \sim 0\text{ }^{\circ}\text{C}$ at 1M), followed by end-capping with TBDMS-Cl, to give the pre-polymer \mathbf{P}_0 . The
 3 monomer:initiator ratio was fixed at 10:1 in all polymerizations to give short oligomers, because
 4 previous work has shown this chain length regime to be the most promising for nontoxic
 5 antibacterials.



6
 7 **Figure 1.** General scheme for the synthesis of self-immolative antibacterial polymers with pendant PEG
 8 and ammonium groups: low-temperature anionic polymerization of a quinone methide monomer, end-
 9 capping, post-polymerization thiol–ene functionalization, and chemically triggered depolymerization with
 10 fluoride.
 11

12 We obtained PBEs with the number-average molecular weights in the range of $M_n = 3.4 -$
 13 3.6 kDa with dispersities of $\mathcal{D} = 1.42 - 1.57$ by GPC. The moderately broad dispersities
 14 observed here are comparable to previous reports on related polymerizations by Phillips⁵¹ and
 15 our group.⁵⁰ Although the “livingness” of this polymerization has not been examined
 16 mechanistically to date, there are two reasonable hypotheses regarding the cause of MWD
 17 broadness; either chain transfer or equilibration of the propagation and depropagation processes

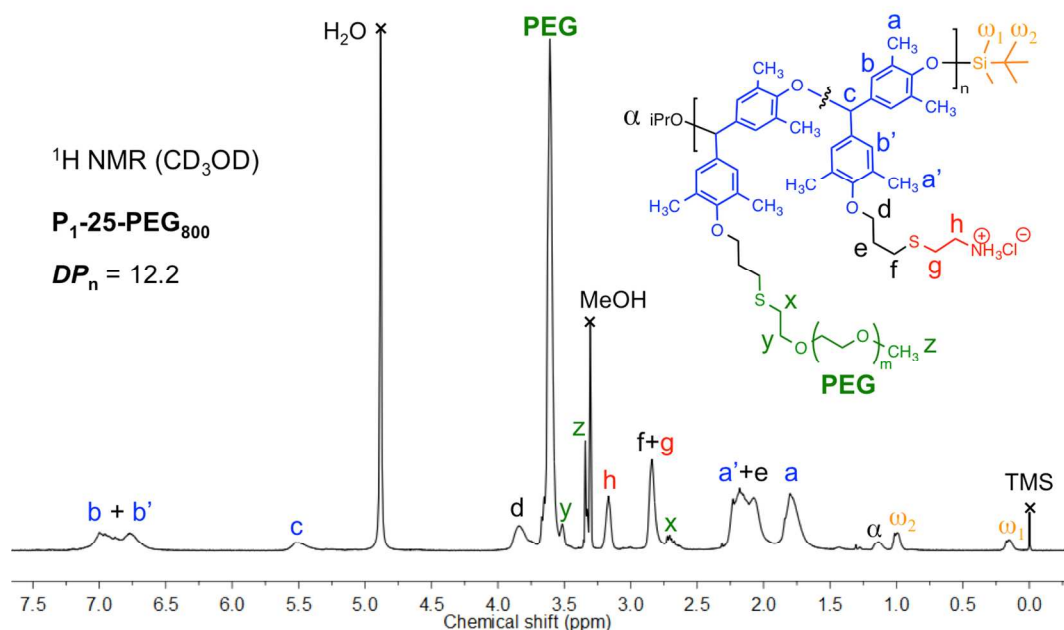
1 following complete conversion. Similar M_n values were found by ^1H NMR end-group analysis
2 (see Supporting Information). The side chains of \mathbf{P}_0 are allyl-functionalized for further
3 modification.

4 The goal of this study was to incorporate neutral, hydrophilic functionality into self-
5 immolative polymers to confer antibacterial activity with minimal hemolytic toxicity. To that
6 end, the allyl side chains of the pre-polymer \mathbf{P}_0 were functionalized with cysteamine HCl (the
7 thiol obtained by cleavage of the disulfide bond in cystamine HCl) and PEG methyl ether thiol
8 (PEG-SH $M_n \sim 800$ Da or 2 kDa) via thiol-ene radical addition. The UV photoinitiator Irgacure
9 651 was employed under irradiation of a handheld UV lamp (6W, 365 nm) for 10 min at room
10 temp. In order to control the ratio of PEG and primary amines in the side chains, we first
11 functionalized a fraction of the allyl side groups with PEG thiols, confirmed the partial
12 conversion by ^1H NMR (see data in ESI), and then proceeded to functionalization of the
13 remaining unreacted allyl groups with excess cysteamine HCl. Each copolymer was purified by
14 preparative size exclusion chromatography on LH-20 gel in MeOH. Copolymer compositions
15 and number-average chain lengths were quantified by ^1H NMR for the final copolymer products
16 (Figure 2). See the SI for spectra of all polymers. We successfully obtained graft copolymers
17 across the full range of copolymer compositions (from 0 to 100 mol% PEG). In all cases, the
18 observed copolymer composition is in good agreement with the target values (data in ESI).

19 All of the functionalized copolymers dissolve in polar solvents such as MeOH, DMF and
20 DMSO. Whereas the copolymers containing 0-33% PEG₈₀₀ are not soluble in aqueous buffers,
21 the copolymers with 50% or more PEG₈₀₀ in side chains demonstrated facile water solubility (up
22 to 1 mg/mL). This observation is consistent with the idea that PEGylation alleviates the intense
23 hydrophobicity of the PBE scaffold. Each copolymer was serially diluted in 2-fold increments

1 from a DMSO stock solution (20 mg/mL) into aqueous buffers to give final polymer
 2 concentrations in the $\mu\text{g/mL}$ range, which is the desired range for our biological assays. As a
 3 control experiment, we confirmed that the residual amount of DMSO (maximum 5% v/v in assay
 4 condition) had no significant effect on bacterial cell viability or on hemolytic activity.

5



6

7 **Figure 2.** ^1H NMR spectrum (CD_3OD) of **P₁-25-PEG₈₀₀**. Copolymer composition and degree of
 8 polymerization are calculated based on the ratios of integrated peak areas.

9

10 **Dye-Labeled Polymers.** We also prepared PBEs end-capped with Rhodamine NHS ester, in
 11 order to enable their observation by confocal fluorescence microscopy (Figure 5A and B), as
 12 well as to aide in quantification of the water-octanol partition coefficients [$\log P =$
 13 $\log([\text{polymer}]_{\text{octanol}} / [\text{polymer}]_{\text{water}})]$, a standard measure of hydrophobicity that is widely used as
 14 a metric in structure-activity relationship (SAR) studies. Positive $\log P$ values indicate a
 15 preference for solubility in octanol, whereas negative values indicate preference for the water
 16 phase. These dye labeled polymers were functionalized with cysteamine and PEG-SH in various

1 ratios (0, 50, and 100% PEG) by the same methods
2 as above. Our hypothesis was that PEGylation
3 would reduce the overall hydrophobicity of the
4 copolymers. Indeed, the logP values exhibit a
5 marked dependence on PEG fraction. The logP
6 values for copolymer containing 0, 50, and 100%
7 PEG₈₀₀ in the side chains are +0.26, -0.56, and
8 -1.20, respectively (Figure 3). Thus, the

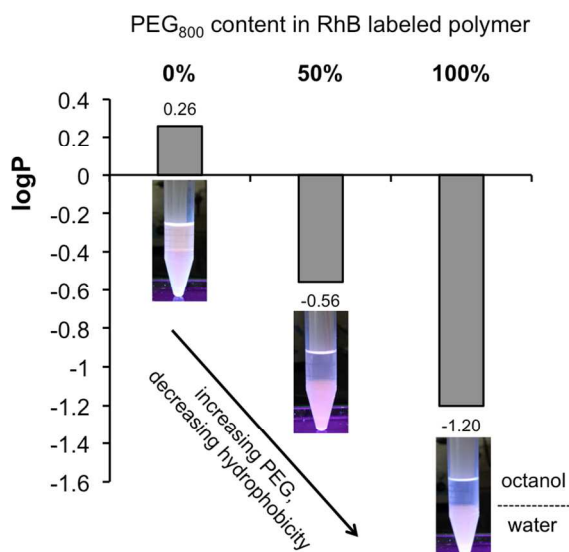


Figure 3. Water-octanol partition coefficients (logP) for the Rhodamine-labeled polymers with 0, 50, and 100% PEG₈₀₀ in the side chains.

9 hydrophobicity trend is quite clear: increasing the
10 PEG content leads to markedly increased
11 hydrophilicity in the copolymers, which strongly supports of the central hypothesis driving this
12 work. Encouraged by this result, we proceeded to perform SAR studies on this class of polymers.
13

14 **Bactericidal activity.** The minimum bactericidal concentration (MBC) is defined here as the
15 lowest polymer concentration required to induce at least a 3-log reduction in the number of
16 viable *E. coli* cells in PBS buffer after 90 min incubation at 37 °C. We quantified the effect of
17 PEGylation extent, as well as the length of the pendant PEG chains, on bactericidal activity
18 (Table 1 and Figure 4). The cationic homopolymer, bearing 100% primary ammonium side
19 chains (**P₁-0**), exhibited potent bactericidal action against *E. coli* with a MBC of 12 µg/mL,
20 which is similar to the MBC of the bee venom toxin melittin (MBC = 4 µg/mL) in the
21 same assay conditions. In our earlier study, we reported similar polymers as strong bactericides
22 with a high degree of cationic charge and hydrophobicity via surfactant-like mode of action.

23 To dilute the high degree of cationic charge and partially screen the hydrophobicity of the

1 PBE backbone, we grafted hydrophilic PEG
 2 chains onto a fraction of the PBE side chains.
 3 Incorporation of modest amounts of PEG₈₀₀
 4 (11 and 25 mol %) did not significantly alter
 5 the antibacterial potency, with MBC values of
 6 26 $\mu\text{g/mL}$. Further increasing the PEG content
 7 (33 and 50 mol %) resulted in MBC values of
 8 12 $\mu\text{g/mL}$, which is unchanged relative to the
 9 cationic homopolymer. Although PEGylation
 10 reduces the hydrophobicity and cationic
 11 charge of the copolymers, the improved
 12 aqueous solubility of the PEGylated
 13 copolymers is a countervailing effect that may
 14 offset the reduced electrostatic interaction
 15 with bacterial membranes⁶². Further increases
 16 in the PEG₈₀₀ content (beyond 50%) lead to a
 17 dramatic loss of antibacterial potency; the

18 copolymer with 57 mol% PEG₈₀₀ has a modest MBC value of 219 $\mu\text{g/mL}$ and those with 63
 19 mol% or higher do not measurably kill *E. coli* even at the highest concentration tested (1000
 20 $\mu\text{g/mL}$).

21 The size effect of grafted PEG chains on antibacterial activity is rather pronounced. When
 22 PEG_{2k} is employed instead of PEG₈₀₀, the antibacterial potency decreases monotonically with
 23 increasing PEG content across the entire range of copolymer compositions (0-100%). Inclusion

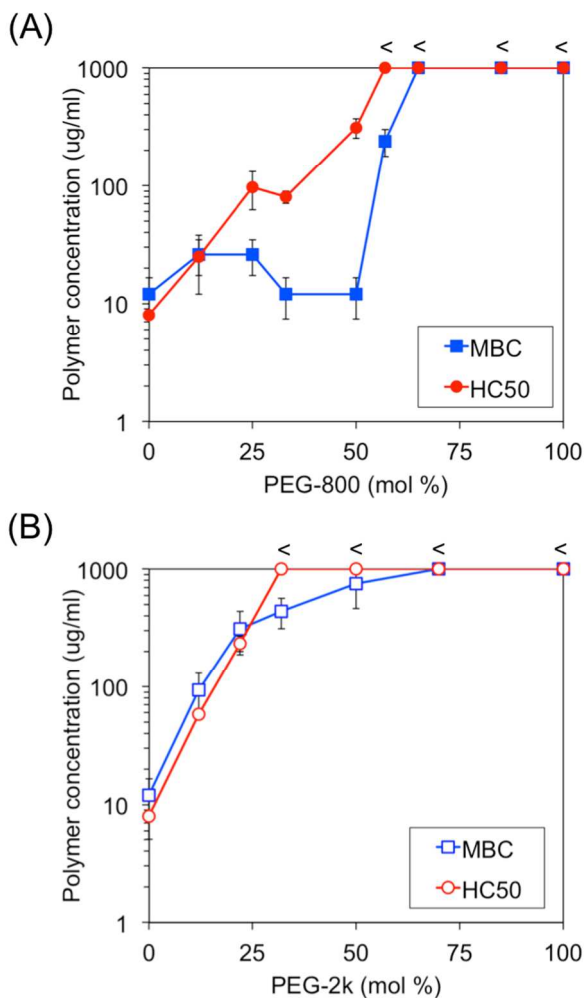


Figure 4. Antibacterial activity and hemolytic activities of polymers with varying mole % of (A) PEG-800 and (B) PEG-2k, as a function of PEG content.

1 of just 12 mol% PEG_{2k} in side chains caused an increase in the MBC to 94 $\mu\text{g/mL}$, compared to
 2 the cationic homopolymer MBC of 12 $\mu\text{g/mL}$ (~8-fold change). Further increasing PEG_{2k}
 3 content significantly abrogated the antibacterial activity, leading to MBC values on the order of
 4 some hundreds of $\mu\text{g/mL}$. Copolymers containing 50 mol% or more of PEG_{2k} are completely
 5 inactive against *E. coli* even at the highest concentration tested (1000 $\mu\text{g/mL}$). The simplest
 6 explanation for this trend is that longer PEG_{2k} chains excessively shield the cationic charge and
 7 backbone hydrophobicity of the polymers, thus deterring the interaction between polymers and
 8 cell membranes to a greater extent than the shorter PEG₈₀₀ chains.

9
 10 **Table 1.** Summary of antimicrobial and hemolytic activities of
 11 cationic amphiphilic poly(benzyl ether)s as a function of molar
 12 percent PEGylation and PEG chain length.
 13

| Polymer | mol% PEG | DP* | MBC <i>E. coli</i> ($\mu\text{g/mL}$) | HC ₅₀ ($\mu\text{g/mL}$) | HC ₅₀ / MBC |
|---|-------------|-----------|---|--|---------------------------|
| P ₁ -100-PEG ₈₀₀ | 100 | 10 | >1000 | >1000 | -- |
| P ₁ -85-PEG ₈₀₀ | 85 | 12 | >1000 | >1000 | -- |
| P ₁ -63-PEG ₈₀₀ | 63 | 11 | >1000 | >1000 | -- |
| P ₁ -57-PEG ₈₀₀ | 57 | 11 | 219 | >1000 | > 4.6 |
| P₁-50-PEG₈₀₀ | 50 | 12 | 12 | 340 | 28.3 |
| P ₁ -33-PEG ₈₀₀ | 33 | 12 | 12 | 83 | 6.9 |
| P ₁ -25-PEG ₈₀₀ | 25 | 12 | 26 | 89 | 3.4 |
| P ₁ -11-PEG ₈₀₀ | 11 | 12 | 26 | 25 | 0.96 |
| P ₁ -100-PEG _{2k} | 100 | 13 | >1000 | >1000 | -- |
| P ₁ -70-PEG _{2k} | 70 | 13 | >1000 | >1000 | -- |
| P ₁ -50-PEG _{2k} | 50 | 11 | 750 | >1000 | >1.3 |
| P ₁ -34-PEG _{2k} | 34 | 12 | 438 | >1000 | >2.3 |
| P ₁ -22-PEG _{2k} | 22 | 12 | 313 | 234 | 0.8 |
| P ₁ -12-PEG _{2k} | 12 | 11 | 94 | 46 | 0.5 |
| P ₁ -0** | 0 | 13 | 12 | < 8 | < 0.7 |
| M ₂ | 100 | -- | >1000 | >1000 | -- |
| M ₁ | 0 | -- | 31 | 62 | 2 |
| DP ₁ -50-PEG ₈₀₀ (+ CsF) | 50 | -- | 8 | 104 | 13 |

14 *Degree of polymerization (DP) from ¹H NMR end group analysis.

15 **Data from reference⁵⁰ for comparison.
 16

1 It is widely understood that “amphiphilic balance” – finely tuning the interplay of cationic
2 charge to hydrophobic character – is central to the design rationale for antibacterial polymers.⁶³
3 ⁶⁴ Overall, the results here show that PEGylation is an effective strategy to influence the
4 “amphiphilic balance” of cationic, amphiphilic polymers, although judiciously tuning the PEG
5 content and PEG chain length is clearly required. This stands in accord with literature precedent
6 on other polymer platforms.^{61, 62} The optimal formulation identified in this work is the copolymer
7 containing ~50% PEG₈₀₀, which shows improved solubility and slightly enhanced antibacterial
8 activity relative to the cationic PBE homopolymer (**P₁-0**).

9 We also compared the activity of dye labeled polymers to that of their unlabeled (silyl ether
10 end-capped) counterparts. The MBC values for *RhB-P₁-0*, *RhB-P₁-40-PEG₈₀₀* and *RhB-P₁-100-*
11 **PEG₈₀₀** are 31, 31 and >1000 µg/mL, respectively, which are comparable to **P₁-0**, **P₁-50-PEG₈₀₀**
12 and **P₁-100-PEG₈₀₀** (12, 12, and >1000 µg/mL) Thus we conclude that dye itself has only a
13 marginal effect on the antibacterial activity, differing only by a single 2-fold dilution, and
14 therefore these dye-capped polymers are appropriately representative of the polymer library in
15 this work.

16 **Hemolytic activity.** The toxicity of these copolymers against mammalian cell membranes is
17 quantified in terms of hemoglobin release from sheep red blood cells (RBCs). The hemolytic
18 concentration (HC₅₀) is defined here as the characteristic polymer concentration that induces
19 50% hemolysis after 1 h incubation at 37 °C, as determined by curve fitting to the Hill equation.
20 The cationic homopolymer (**P₁-0**) was markedly hemolytic with an HC₅₀ value lower than 8
21 µg/mL, which is comparable to melittin (HC₅₀ = 6 µg/mL) in the same assay conditions, in
22 agreement with our recent report.⁵⁰ Incorporation of increasing amounts of PEG₈₀₀
23 monotonically increases the HC₅₀ values by orders of magnitude (Table 1 and Figure 4). The

1 addition of just 11 mol% of PEG₈₀₀ in side chains reduced the hemolytic toxicity by ~ 4-fold
2 (HC₅₀ = 25 µg/mL). Further increasing the PEG₈₀₀ content to 25% and 33% mole led to an
3 additional ~3-fold increase in the HC₅₀ (89 µg/mL). This trend continued for copolymers
4 containing up to 50 mol% PEG₈₀₀ (HC₅₀ = 340 µg/mL). Higher PEG₈₀₀ content led to complete
5 loss of hemolytic activity with HC₅₀ values above the highest concentration tested (1000 µg/mL).
6 Cell-type selectivity against bacterial cells without toxicity to mammalian cells is crucial for
7 biomedical-related applications. Comparing the relative magnitudes of HC₅₀ and MBC values for
8 the copolymers in this work reveals that the most promising example thus far is the PBE
9 copolymer containing 50% PEG₈₀₀ (HC₅₀/MBC = 28.3). This metric represents a very marked
10 improvement relative to our first-generation self-immolative antibacterial PBE (HC₅₀/MBC =
11 0.5).⁵⁰ Thus, we report the first example of a cell-type selective antibacterial polymer that
12 possesses the unique self-immolative characteristic.

13 Incorporation of longer grafted PEG_{2k} in side chains exhibited similar effect on hemolytic
14 activity; higher degrees of PEG substitution are associated with loss of hemolytic toxicity in a
15 monotonic manner. The slope of the HC₅₀ versus PEG mol% plot (Figure 4) is higher for PEG_{2k}
16 than for PEG₈₀₀, implying that the longer PEG chains impact the activity more significantly in
17 the low PEG content regime. For example, incorporation of 12 mol% PEG_{2k} gave an HC₅₀ value
18 of 46 µg/mL, which is about 6-fold higher than the cationic homopolymer **P1-0** and about 2-fold
19 less hemolytic than the copolymer containing about the same molar percent of PEG₈₀₀.
20 Increasing PEG_{2k} mole content to 20% further decreased hemolytic activity. All polymers having
21 34% or more of PEG_{2k} in the side chains were non-hemolytic even at maximum concentration
22 tested, 1000 µg/mL. Comparing two polymers with similar % mole of PEG, it is obvious that
23 those with longer PEG_{2k} units showed much more hemocompatibility relative to polymer bearing

1 shorter PEG₈₀₀. For example, **P₁-34-PEG_{2k}** has an HC₅₀ > 1000 μg/mL, compared to **P₁-33-**
2 **PEG₈₀₀**, which has HC₅₀ = 83 μg/mL (a difference of more than 12-fold). The effect again can be
3 explained by backbone screening by the longer grafted PEG chains, which shields the potent
4 hydrophobicity of the benzyl ether backbone, thus diminishing the interactions with RBC lipid
5 bilayers. Even though polymers with longer PEG side groups are non-hemolytic, they are also
6 less potent antibacterial agents, and hence do not confer excellent selectivity. The best cell-
7 selectivity for a copolymer bearing PEG_{2k} was a modest HC₅₀/MBC > 2.3 for the polymer with
8 34 mol% PEG_{2k}. This value is far lower than the best example from the PEG₈₀₀ series, which was
9 HC₅₀/MBC = 28.3. It is thus reasonable to speculate that even shorter PEGs may have an even
10 greater effect on the enhancement of selectivity, although at some point the palliative effect is
11 expected to diminish.

12 In contrast to negatively charged bacterial cell surfaces, the outer leaflet of the phospholipid
13 bilayer in the RBC membrane displays a lower density of anionic charges.^{6, 26} The hemolytic
14 behavior of amphiphilic polymers has thus been mostly associated with their hydrophobicity,
15 which results in membrane binding and surfactant-like disruption⁶⁵. The incorporation of
16 hydrophilic PEG side chains plays a prominent role in dictating the hemolytic activity of
17 synthetic polymers. Plasma proteins in blood adsorb on RBCs and protect them from external
18 stresses. In the absence of blood plasma, RBCs become more delicate and susceptible to lytic
19 agents (such as in PBS, the assay media used here).⁶⁶ PEG also behaves as a protective agent by
20 shielding cells from foreign body contact. It has been shown that PEG weakly adsorbs to the cell
21 membrane via hydrogen bonding to improve protection through cells⁶⁷. Consequently, polymers
22 containing PEG may also reduce hemolytic toxicity by these or related mechanisms, in addition
23 to its role in reducing the overall hydrophobicity of the copolymers.

1 **Broad Spectrum and Kinetics.** The most promising candidate identified in our initial screen
 2 was the copolymer containing 50 mol% PEG₈₀₀ and 50 mol% cysteamine in the side chains, **P₁-**
 3 **50-PEG₈₀₀**. We further examined the bactericidal profile of this select formulation in terms of
 4 broad-spectrum activity and bactericidal kinetics (Figure 5). The copolymer does exert
 5 bactericidal activity against both Gram-positive and Gram-negative bacteria. Bactericidal activity
 6 is generally more potent in the case of Gram-
 7 negatives; the MBC values against *E. coli* and *P.*
 8 *aureginosa* are 12 and 4 µg/mL, respectively,
 9 whereas against *S. aureus* and *E. faecalis* the values
 10 are 250 and 125 µg/mL. This observation is similar
 11 to our previous findings with PBE cationic
 12 homopolymers, which exerted much more potent
 13 activity against Gram-negatives as compared to
 14 Gram-positives. In addition, it was found that the
 15 kinetics are slower against Gram- positives,
 16 requiring 4-hr incubation to induce a 4-log reduction
 17 in the number of viable *S. aureus* cells (99.99%
 18 killing) as opposed to less than 1-hr in the case of *E.*
 19 *coli*. It is interesting that these PEGylated PBEs
 20 generally show better activity against Gram negative
 21 strains relative to Gram positives. Indeed, many
 22 examples of antibacterial polymers are more active
 23 against Gram-positive bacteria relative to Gram-

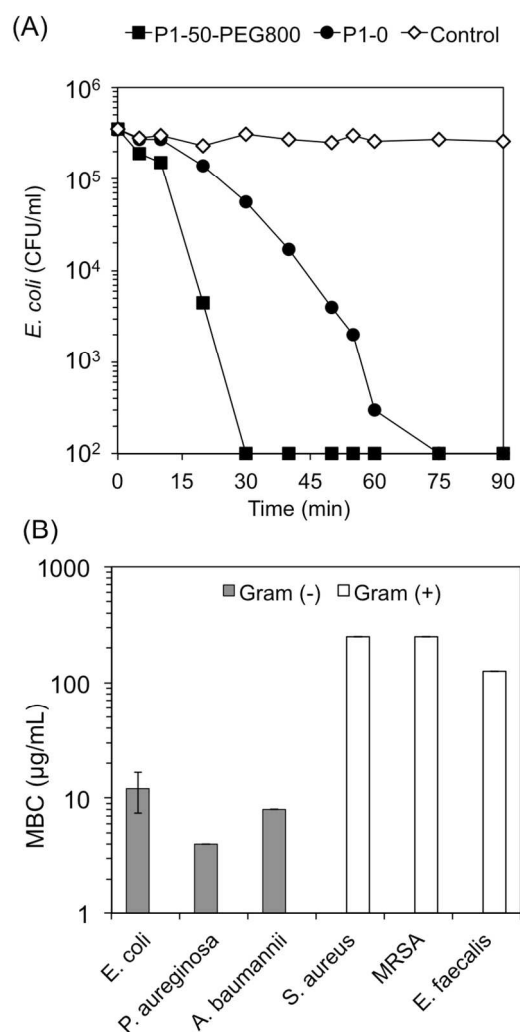


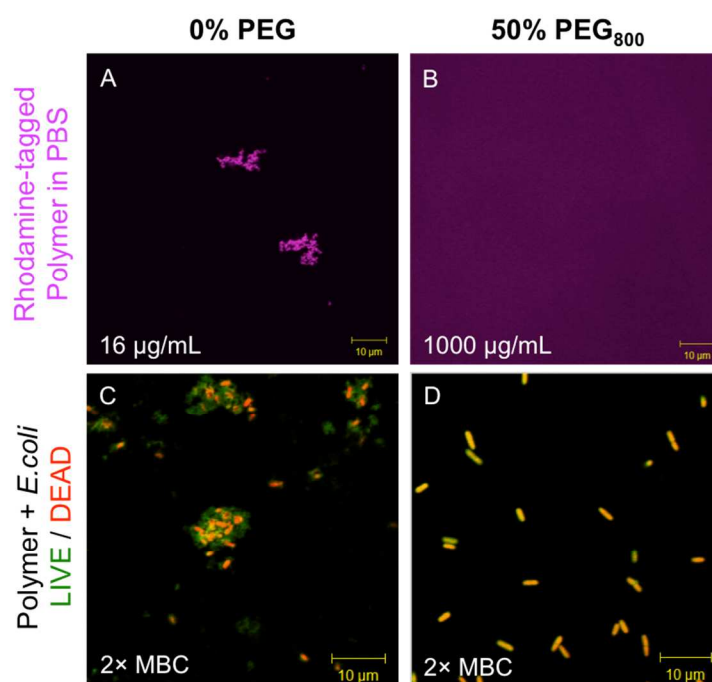
Figure 5. (a) Bactericidal kinetics of **P₁-0** and **P₁-50-PEG₈₀₀** against *E. coli* in PBS at 2×MBC and (b) Broad spectrum activity against Gram-positive and -negative bacteria.

1 negatives, although there are also examples that show the opposite preference.⁶⁸ A study by
2 Lienkamp *et al* found that there may also be a molecular sieving effect of the peptidoglycan layer
3 in Gram positives.⁶⁹ The details of the mechanism of action are outside the scope of this work,
4 but we hypothesize that the thick, cross-linked peptidoglycan layer present in Gram positives
5 may be difficult for these PBE-*graft*-PEG copolymers to translocate.

6 The PEGylated copolymer **P₁-50-PEG₈₀₀** exerts markedly faster bactericidal kinetics against
7 *E. coli* (4-log reduction in < 30 min) relative to the cationic homopolymer **P₁-0** (~ 90 min), as
8 shown in Figure 4A. This observation initially seems counterintuitive because the PEGylated
9 copolymer has a lower cationic charge density and lower hydrophobicity, relative to the cationic
10 homopolymer, and the membrane disruption is thought to depend on both electrostatic and
11 hydrophobic interactions. We hypothesized that the PEGylated polymer acts faster overall due to
12 the more subtle hydrophobicity, which disfavors aggregation in solution and thus may facilitate
13 the binding of individually solvated polymer chains onto the bacterial cell envelope. In contrast,
14 the excessively hydrophobic **P₁-0** may exist as aggregates in solution that display cationic groups
15 on the surface and bury the hydrophobic residues in an inner globule. This sort of hydrophobic
16 clustering hypothesis has been invoked to explain the reduced antibacterial activity in the case of
17 excessively hydrophobic polymethacrylates.⁷⁰

18 To probe our hypothesis, we used the Rhodamine-labeled variants of **P₁-0**, **P₁-50-PEG₈₀₀**,
19 and **P₁-100-PEG₈₀₀** each containing one dye tag in the terminal end group (see ESI for synthetic
20 details). The MBC values of these tagged polymers are similar to the untagged polymers of same
21 copolymer composition (data in ESI). Indeed, confocal microscopy images of the *RhB*-**P₁-0** show
22 micron-sized aggregates in PBS buffer at concentrations as low as 16 µg/mL (Figure 6A), which
23 is similar to the MBC value. In stark contrast, *RhB*-**P₁-50-PEG₈₀₀** and *RhB*-**P₁-100-PEG₈₀₀** both

1 show diffuse, uniform fluorescence intensity in PBS even up to 1000 $\mu\text{g/mL}$, which is well
2 above the MBC value (Figure 6B). A detailed study on the polymer aggregates using Dynamic
3 Light Scattering (DLS) is beyond the scope of this work, but may be an interesting avenue for
4 future work.



5
6
7 **Figure 6.** Confocal images of (A, B) rhodamine dye-labeled polymers in PBS media and (C, D) non-labeled
8 polymers at 2x MBC with *E. coli* and LIVE/DEAD stains.

9
10 Moreover, when the Rhodamine-labeled polymers are mixed with *E. coli* cells, there is a very
11 clear localization of *RhB-P₁-50-PEG₈₀₀* specifically on the cell membrane observed in the
12 confocal images (Figure 7A). In contrast, when *RhB-P₁-0* is mixed with the *E. coli* cells,
13 aggregates on the order of 10-30 microns are observed, with no clear individual rod-shaped
14 bacteria cells (Figure 7B). These data strongly support the notion that the activity of the cationic
15 homopolymer *P₁-0* is indeed hampered by extensive polymer-polymer aggregation in aqueous
16 media, as we expected. The PEGylation strategy indeed alleviates the excessive hydrophobicity

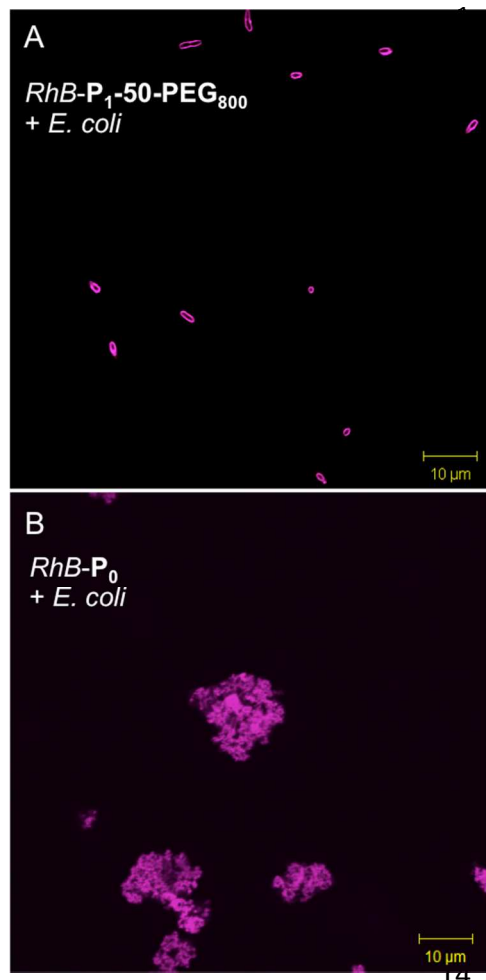


Figure 7. (A) Rhodamine-labeled polymer with 50% PEG₈₀₀ in the side chains binds specifically to the membranes of individual planktonic *E. coli* cells, seen as bright emission from the outlines of smooth rod-shaped cells. (B) Rhodamine-labeled polymer with no PEG (all cysteamine side chains) shows only indistinct aggregates.

of the PBE backbone and brings the global physiochemical properties of the copolymer into the appropriate range for “amphiphilic balance” required to give favorable biological activity.

Triggered depolymerization. We next examined the influence of specifically triggered depolymerization on the antibacterial and hemolytic activities of PEGylated cationic PBEs. In accord with our prior work, TBDMS-capped pre-polymers (**P₀**) undergo rapid depolymerization to small molecules upon fluoride exposure, evidenced by ¹H NMR and GPC⁵⁰. In this work, fluoride was introduced as an exogenous trigger. In general, the PBE platform boasts a great deal of diversity in terms of end-cap/trigger combinations that can be used to mediate self-immolation. The present example was selected for synthetic accessibility and because the

fluoride ion is biologically *inactive* against bacterial and human cells. Indeed, we are also interested in expanding this work to include naturally occurring *endogenous* triggering chemistries, perhaps involving natural changes in redox, pH, or enzymatic cues, but these efforts are outside the scope of the present work.

Triggered depolymerization of **P₁-50-PEG₈₀₀** was initiated by cesium fluoride (CsF) in MeOH or DMF, and monitored by ¹H NMR and GPC (Figure 8). Upon F⁻ treatment, broad

1 features in the ^1H NMR spectra attributed to the PBE backbone disappeared and were replaced
2 by sharp peaks corresponding to small molecule products of depolymerization. The
3 disappearance of the resonance at ~ 5.5 ppm is used to quantify the percentage of
4 depolymerization, which reached completion after stirring overnight (Figure S35, ESI). The GPC
5 trace (in DMF) also shows a corresponding shift to longer retention times, in accord with
6 products of smaller hydrodynamic volume that match the chromatogram for the PEG₈₀₀ grafted
7 monomer **M**₂. The MBC for intact polymer **P**_{1-50-PEG}₈₀₀ was 12 $\mu\text{g}/\text{mL}$. In response to
8 fluoride, **P**_{1-50-PEG}₈₀₀ degraded into its small molecule components (referred to as **DP**₁₋₅₀₋
9 **PEG**₈₀₀ in Table 1), which had an MBC value of 8 $\mu\text{g}/\text{mL}$. Thus, the products of
10 depolymerization appeared to exert similar antibacterial activity than the intact polymer. The
11 small change in MBC upon depolymerization is consistent with the observation that the small
12 molecule product of depolymerization containing an ammonium cation is a potent antibacterial
13 agent, although the PEGylated monomer has no antibacterial activity.

14 We also investigated the biological activities of model small molecule compounds that
15 contain either primary amine (**M**₁ in Table 1) or PEG₈₀₀ (**M**₂) attached to a single unit of the
16 bisphenol (chemical structures given in Figure 1) as a standard for comparison. In contrast to the
17 potent antibacterial activity of the primary amine functionalized monomer **M**₁ (31 $\mu\text{g}/\text{mL}$), the
18 PEGylated monomer **M**₂ was inactive against *E. coli* up to 1000 $\mu\text{g}/\text{mL}$.

19

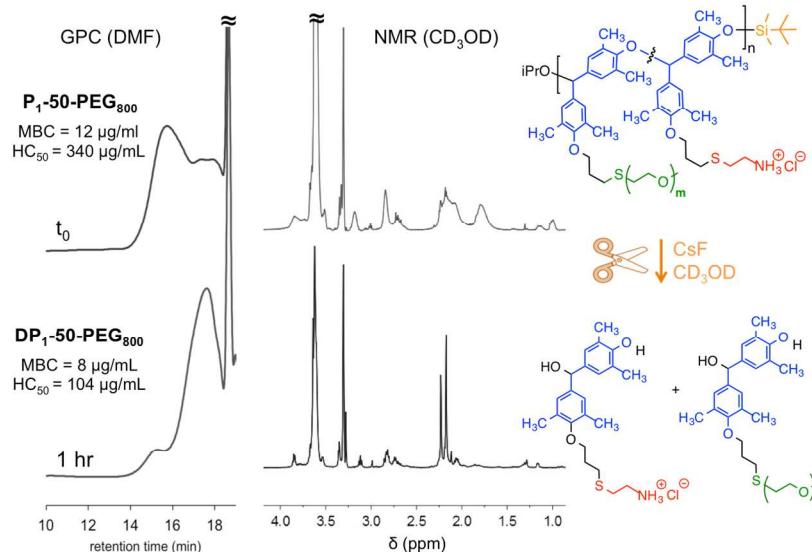


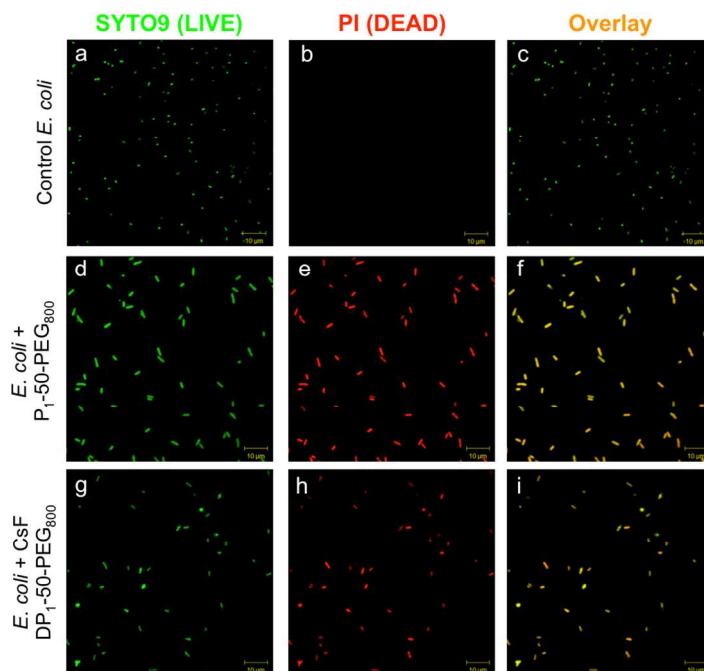
Figure 8. ^1H NMR (CD_3OD) and GPC (DMF) of $\text{P}_1\text{-50-PEG}_{800}$ before and after CsF in MeOH, with their corresponding chemical structures and biological activities.

Triggered self-immolation also influences the hemolytic activity compared to intact polymer.

For example, $\text{P}_1\text{-50-PEG}_{800}$ ($\text{HC}_{50} = 340 \mu\text{g/mL}$) depolymerized into $\text{DP}_1\text{-50-PEG}_{800}$ ($\text{HC}_{50} = 104 \mu\text{g/mL}$), about a 3-fold change. This result can be understood in terms of the HC_{50} values for the two monomer components: $62 \mu\text{g/mL}$ for M_1 and $>1000 \mu\text{g/mL}$ for M_2 . If one considers that the two are present in approximately a 1:1 ratio (for this 50-50% copolymer), and that one component is completely inactive, then we expect the simple mixture to have an HC_{50} value that is simply double that of the active component ($2 \times 62 = 124 \mu\text{g/mL}$). The experimental result is $104 \mu\text{g/mL}$, which is in reasonably good agreement with the prediction for a simple mixture. Slight differences may be due to the presence of some amount of dimeric species, which has been observed previously in the depolymerization byproducts for PBE.⁵⁰

In addition to the MBC assay that quantified cell death in terms of the number of viable colonies observable to the unaided eye, we also evaluated the antibacterial activity of polymers and its small components by confocal laser scanning microscopy to visualize the antibacterial

1 effect at the individual cell level, before and after depolymerization (Figure 9).



2
3 **Figure 9.** Confocal images of *E. coli* cells (a–c) alone, (d–f) after exposure to **P₁-50-PEG₈₀₀**, (g–i) after
4 exposure to CsF-depolymerization products **DP₁-50-PEG₈₀₀**. Scale bar is 10 μm in all images. Additional
5 images of cells treated with **M₁** and **M₂** are in the SI.
6

7 For this study, we employed the commercially-available BacLight LIVE/DEAD staining kit,
8 which includes the proprietary SYTO9 dye (green) that stains both live and dead cells
9 indiscriminately, and propidium iodide (PI, red) that emits only when intercalated into DNA
10 within the cytoplasm.⁷¹ PI staining is thus used as a metric to confirm the permeabilization of the
11 cell membrane, which is the putative mechanism of action for cationic, amphiphilic antibacterial
12 agents.^{72–76} Firstly, as a positive control, *E. coli* cells in the absence of polymers were examined.
13 In confocal images, we observed smooth, rod-shaped *E. coli* cells in the green SYTO9 channel
14 with no detectable emission in the red PI channel, which suggests healthy live cells (Figure 9 a-
15 c). To assess the impact of the polymers, *E. coli* (5×10^7 CFU/mL) was incubated for 90 min at 37
16 °C in the presence of antibacterial polymers above their lethal concentration ($4 \times \text{MBC}$). We

1 examined both the intact copolymer **P₁-50-PEG₈₀₀** (Figure 9 d-f) as well as the products of the
2 triggered depolymerization **DP₁-50-PEG₈₀₀** (Figure 9 g-i). Both samples showed bright emission
3 in the green and red channels, suggesting substantial co-localization of both fluorophores within
4 the cells.

5 Based on the fact that the PI stain cannot translocate healthy cell membranes, combined with
6 specific membrane stained by our Rh-labeled polymers, we conclude that DNA-intercalated PI
7 stain within the cytoplasm is associated with a deterioration of the cell membrane barrier
8 function upon exposure to antibacterial polymers. Thus, it would appear that the polymers in this
9 work are capable of permeabilizing the *E. coli* cells, in accord with numerous other literature
10 examples on cationic, amphiphilic polymers.⁷²⁻⁷⁶

11 The primary amine functionalized model monomer **M₁** also showed extensive PI staining
12 within the cells (images in ESI). On the other hand, monomer with PEG₈₀₀ functionality **M₂** did
13 not induce any red PI emission from cells, which again confirms that the PEG₈₀₀ monomer units
14 are not bactericidal (images in ESI). Interestingly, the confocal images in this work are rather
15 different in appearance relative to our previous report on the cationic homopolymer. Whereas **P₁-**
16 **0** showed red PI staining of large cell-cell aggregates on the order of several tens of microns
17 (Figure 6C),⁵⁰ the PEGylated variants in the present study appear to stain cells individually
18 without inducing extensive cell-cell aggregation (Figure 6D and 7B), which is also consistent
19 with the concept of reduced hydrophobicity (more negative logP values) for the PEGylated
20 polymers.

21 **Control Experiments.** The CsF was not removed prior to testing the biological activity; CsF
22 showed no effect on *E. coli* cell viability even at concentrations 10× higher than present in the
23 assays. As a negative control for triggering, PBEs were end-capped with inert methyl groups,

1 side-chain functionalized and exposed to CsF under same conditions. The fluoride-triggered
2 depolymerization did not occur in those polymers, evidenced by ^1H NMR, and tested for MBC
3 and HC_{50} . Before and after CsF exposure, MBC and HC_{50} values did not show any significant
4 changes. Hence, we confirmed that fluoride-triggered depolymerization is specific to silyl ether
5 end-capped polymers. In addition, we confirmed that no adverse side reactions occur when the
6 allyl functionalized pre-polymer \mathbf{P}_0 is exposed to cysteamine (or PEG-SH) under UV irradiation
7 with no photoinitiator present. Similarly, no reaction is observed when \mathbf{P}_0 and photoinitiator
8 under UV irradiation without any thiol present.

9

10 Experimental

11 **Materials and Methods.** Reagents were purchased commercially and used as received without further
12 purification unless noted. 4,4'-methylenebis(2,6-dimethylphenol) was purchased from Tokyo Chemical Industry
13 (TCI America, USA). Potassium carbonate (K_2CO_3), allyl bromide (allyl Br), ammonium chloride (NH_4Cl), sodium
14 chloride (NaCl), anhydrous sodium sulfates (Na_2SO_4), silver oxide (Ag_2O), tert-butyldimethylsilyl chloride
15 (TBDMS-Cl), imidazole, 2-aminoethanethiol hydrochloride (cysteamine), poly(ethylene glycol) methyl ether thiol
16 ($M_n = 800\text{g/mole}$ and $M_n = 2000\text{ g/mole}$), 2,2-dimethoxy-2-phenylacetophenone (DMPA), cesium fluoride (CsF),
17 Triton X-100, sodium phosphate monobasic monohydrate and sodium phosphate dibasic heptahydrate were
18 purchased from Sigma-Aldrich (USA). 1-tert-Butyl-2,2,4,4,4-pentakis(dimethylamino)-2,2,4,4,4-
19 catenadi(phosphazene) (P_2 -*t*-Bu base) (2.0 M solution in THF) was also purchased from Sigma-Aldrich and stored
20 in a glove box under N_2 atmosphere. BacLight™ Bacterial Viability Kit L-7007 and NHS-Rhodamine (5/6-carboxy-
21 tetramethyl-rhodamine succinimidyl ester) were purchased from Thermo Fisher Scientific (USA). 10% (v/v) red
22 blood cells (RBCs) was obtained from MP Biomedicals (USA). Organic solvents: diethyl ether (Et_2O), N,N-
23 dimethylformamide (DMF), ethyl acetate, hexane, methanol (MeOH), and dimethyl sulfoxide (DMSO) were
24 obtained from Sigma-Aldrich (USA). Isopropanol (iPrOH) was distilled before use. Anhydrous tetrahydrofuran
25 (THF) was obtained from solvent purification system. Deionized water was purified using EDM Millipore
26 purification system. Sephadex LH-20 was obtained from Sigma-Aldrich. Flash-column chromatography was

1 employed using silica gel (60 Å pore size, 40-63 µm technical grade, Sigma-Aldrich). Thin-layer chromatography
2 was performed on IB2-F J.T. Baker silica gel TLC (Germany).

3 Proton nuclear magnetic resonance (^1H NMR) spectra were recorded using 500 MHz Agilent NMR
4 spectrometer at 25 °C. NMR chemical shifts were reported in parts per million (ppm, δ) and referenced to
5 tetramethylsilane ($(\text{CH}_3)_4\text{Si}$, 0.00 ppm) or to residual solvent signals (CDCl_3 (δ 7.27), $(\text{CD}_3)_2\text{OS}$ (δ 2.50), or CD_3OD
6 (δ 3.31 and 4.78). Carbon nuclear magnetic resonance (^{13}C NMR) spectra were recorded using 500 MHz Agilent
7 NMR spectrometer at 25 °C. NMR chemical shifts were reported in parts per million (ppm, δ) and referenced to
8 residual solvent signals (CDCl_3 (δ 77.0), or CD_3OD (δ 49.0)).

9 Size exclusion chromatography (SEC) was performed on Agilent Technologies 1260 Infinity GPC system
10 equipped with a refractive index detector and PLGel columns using THF and DMF as the mobile phase (flow rate: 1
11 mL/min, 25 °C for THF, flow rate: 1 mL/min, 45 °C for DMF). Molecular weight was calibrated using
12 monodisperse polystyrene standards.

13 Laser scanning confocal microscopy (Zeiss LSM 510 Meta) was employed using Argon (458-488-514 nm) and
14 HeNeI (543 nm) lasers. 512 x 512 pixel images were recorded from single scan.

15 Mass spectra were measured on Thermo LTQ XL Orbitrap mass spectrometer (Thermo, Bremen, Germany)
16 with electrospray ionization ion source. Samples were injected using an Agilent 1200 nano-HPLC system (Agilent,
17 Palo Alto, CA) using an Agilent 1200 autosampler. The flow rate of the solvent was 50 µL/min. The injection
18 volume was 1-2 µL. The data were collected in m/z range of 100-900 at the resolution of 30,000. The accuracy of
19 mass measurements was ~3 ppm.

20 **Monomer Synthesis.** Allyl Br (1.0 equiv) was added dropwise to a stirred mixture of 4,4'-methylenebis(2,6-
21 dimethylphenol) (1.0 equiv) and K_2CO_3 (1.1 equiv) in DMF (0.4 M). After 24 h reaction at room temperature, the
22 mixture was extracted with ethyl acetate and deionized H_2O . The organic layer was washed with saturated NH_4Cl
23 solution and then brine. It was dried over anhydrous Na_2SO_4 , filtered to separate salts and concentrated via rotary
24 evaporation. On TLC plate, there were three spots observed, assigned to compounds with double allyl and single
25 allyl in the side chains, and unreacted starting material. The viscous oil was purified by silica gel column
26 chromatography with gradient elution of solvents (10 – 33% ethyl acetate in hexanes) to afford compound with
27 **single allyl** as a yellow oil (yield 28%).

28 Ag_2O (2.0 equiv) was added into the solution of **single allyl** compound (1.0 equiv) and Et_2O (0.1 M). The

1 reaction was stirred for 16 h at room temperature. The mixture was filtered to remove silver oxide particles,
2 concentrated via rotary evaporator and recrystallized in hot cyclohexane to afford yellow crystals. The monomer M_0
3 crystals were ground and dried in vacuum for 72 h. Dry monomer (67%) was store in an inert glovebox atmosphere.

4 **Polymer Synthesis.** The monomer M_0 (1.0 equiv) was dissolved in anhydrous THF. A stock solution of distilled
5 iPrOH (0.1 equiv) and 2.0 M P_2 -*t*-Bu base solution (0.1 equiv) in THF was prepared in anhydrous THF (1:1 ratio).
6 The chain length of polymer was tuned by altering the number of equivalents of initiator relative to monomer. Based
7 on that, certain amount of initiator-base stock solution was added into monomer solution to pre-initiate and stirred
8 for 1 h at room temperature. Final concentration of reaction was adjusted to 0.8 M. The reaction became dark red
9 from bright yellow color after the addition of base. Following the initiation, polymerization was conducted in -20 °C
10 for 4 h with stirring. All steps were carried out in glovebox under inert N_2 environment.

11 **End-capping.** TBDMS-Cl (1.0 equiv) and imidazole (1.0 equiv) were dissolved in anhydrous THF and then
12 injected into polymer reaction at -20 °C which immediately turned into orange-yellow color from dark red. Reaction
13 was stirred for 24 h at -20 °C. It was allowed to warm to room temperature and continued to stir at this temperature
14 for few hours. The polymer was precipitated in MeOH and collected via centrifuge. Excess MeOH was decanted.
15 The polymer was redissolved in THF and precipitated in MeOH and centrifuged again, whole process was repeated
16 three times. Polymers were dried in vacuum for 24 h. Yields for each polymerization are given in the ESI.

17 Synthetic procedures largely followed the precedent by Phillips,⁵¹ and our own prior report,⁵⁰ with minor
18 modifications. Further synthetic details, triggered depolymerization, NMR and GPC data, biological assay protocols,
19 and microscopy procedures, are included in the Electronic Supporting Information (ESI) document.

20

21 **Conclusions**

22 We functionalized the side chains of a self-immolative poly(benzyl ether) with a combination
23 of cationic ammonium groups and neutral, hydrophilic PEG chains. The antibacterial and
24 hemolytic activity of these copolymers is sensitively dependent on the cationic charge and
25 hydrophobicity of the polymer chains. Here, we find that side chain PEGylation is a highly
26 effective strategy to modulate the hydrophobicity and to enhance cell-type selectivity. The

1 copolymer composition (molar percentage of PEG grafts) and the PEG chain length are key
2 design parameters for tuning biological activity. From our library of PBE copolymers, the most
3 promising example is one that contains 50 mol% PEG₈₀₀ and 50 mol% primary ammonium
4 cationic side chains. This select example exerts excellent 28-fold selectivity for bacterial cells
5 relative to mammalian RBCs. The sensitive and specific self-immolative characteristics of the
6 backbone are retained upon side chain functionalization.

7 In this work, we used stimuli-responsive end-caps that are cleaved on demand by externally
8 applied stimulus, like fluoride ions. The beauty of the self-immolative PBE platform is that these
9 polymers can be designed with a variety of responsive groups, triggered by light, pH, or redox.
10 Currently, we are developing biologically active degradable macromolecules that can be
11 degraded by naturally occurring stimuli including bacterial enzymes. We envision these
12 materials may be useful in a broad range of antibacterial and antibiofilm coatings with unique
13 “triggered-cleaning” characteristics. These and related studies are currently underway in our
14 laboratory.

15

16 **Acknowledgements**

17 We thank Prof. Scott Phillips for helpful discussions on self-immolative polymer synthesis,
18 Prof. Sangwoo Lee and Prof. Chulsung Bae for the use of GPC, Dr. Ao Chen for helpful
19 discussions, and undergraduate students Samuel Ellman, Sadjo Sidikou, and Phillip Falcone for
20 their assistance with the synthesis and scale-up of the monomers used in this study. E.F.P.
21 acknowledges funding from a 3M Non-Tenured Faculty Award, a National Science Foundation
22 CAREER Award (DMR BMAT #1653418), and the American Chemical Society Petroleum
23 Research Fund (57806-DNI7). C.E. was supported in part by a Presidential Graduate Research

1 Fellowship from Rensselaer Polytechnic Institute.

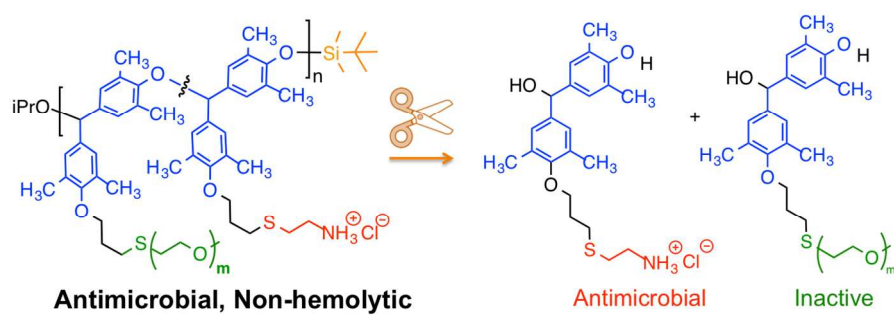
2

3

4

5

ToC Graphic:



6

7

8

9

1 References

- 2
- 3 1. H. W. Boucher, G. H. Talbot, J. S. Bradley, J. E. Edwards, D. Gilbert, L. B. Rice, M. Scheld, B. Spellberg
- 4 and J. Bartlett, *Clin Infect Dis*, 2009, **48**, 1-12.
- 5 2. H. C. Neu, *Science*, 1992, **257**, 1064-1073.
- 6 3. J. Rello, E. Bunsow and A. Perez, *Expert Rev Clin Phar*, 2016, **9**, 1547-1555.
- 7 4. M. Zasloff, *Nature*, 2002, **415**, 389-395.
- 8 5. T. Ganz, *Nature*, 2001, **412**, 392-393.
- 9 6. R. E. W. Hancock and H. G. Sahl, *Nat Biotechnol*, 2006, **24**, 1551-1557.
- 10 7. E. A. Porter, X. F. Wang, H. S. Lee, B. Weisblum and S. H. Gellman, *Nature*, 2000, **404**, 565-565.
- 11 8. J. A. Patch and A. E. Barron, *Journal of the American Chemical Society*, 2003, **125**, 12092-12093.
- 12 9. B. P. Mowery, S. E. Lee, D. A. Kissounko, R. F. Epand, R. M. Epand, B. Weisblum, S. S. Stahl and S. H.
- 13 Gellman, *Journal of the American Chemical Society*, 2007, **129**, 15474+.
- 14 10. K. Kuroda and W. F. DeGrado, *J Am Chem Soc*, 2005, **127**, 4128-4129.
- 15 11. E. F. Palermo and K. Kuroda, *Biomacromolecules*, 2009, **10**, 1416-1428.
- 16 12. E. F. Palermo, S. Vemparala and K. Kuroda, *Biomacromolecules*, 2012, **13**, 1632-1641.
- 17 13. E. F. Palermo, I. Sovadinova and K. Kuroda, *Biomacromolecules*, 2009, **10**, 3098-3107.
- 18 14. W. Chin, G. S. Zhong, Q. Q. Pu, C. Yang, W. Y. Lou, P. F. De Sessions, B. Periaswamy, A. Lee, Z. C.
- 19 Liang, X. Ding, S. J. Gao, C. W. Chu, S. Bianco, C. Bao, Y. W. Tong, W. M. Fan, M. Wu, J. L. Hedrick
- 20 and Y. Y. Yang, *Nat Commun*, 2018, **9**.
- 21 15. W. Chin, C. A. Yang, V. W. L. Ng, Y. Huang, J. C. Cheng, Y. W. Tong, D. J. Coady, W. M. Fan, J. L.
- 22 Hedrick and Y. Y. Yang, *Macromolecules*, 2013, **46**, 8797-8807.
- 23 16. A. C. Engler, J. P. K. Tan, Z. Y. Ong, D. J. Coady, V. W. L. Ng, Y. Y. Yang and J. L. Hedrick,
- 24 *Biomacromolecules*, 2013, **14**, 4331-4339.
- 25 17. F. Nederberg, Y. Zhang, J. P. K. Tan, K. J. Xu, H. Y. Wang, C. Yang, S. J. Gao, X. D. Guo, K. Fukushima,
- 26 L. J. Li, J. L. Hedrick and Y. Y. Yang, *Nature Chemistry*, 2011, **3**, 409-414.
- 27 18. M. F. Ilker, K. Nusslein, G. N. Tew and E. B. Coughlin, *J Am Chem Soc*, 2004, **126**, 15870-15875.
- 28 19. G. J. Gabriel, J. A. Maegerlein, C. E. Nelson, J. M. Dabkowski, T. Eren, K. Nusslein and G. N. Tew,
- 29 *Chem-Eur J*, 2009, **15**, 433-439.
- 30 20. K. Lienkamp and G. N. Tew, *Chem-Eur J*, 2009, **15**, 11784-11800.
- 31 21. C. Ergene, K. Yasuhara and E. F. Palermo, *Polym Chem-Uk*, 2018, **9**, 2407-2427.
- 32 22. Y. C. Yang, Z. G. Cai, Z. H. Huang, X. Y. Tang and X. Zhang, *Polym J*, 2018, **50**, 33-44.
- 33 23. W. Ren, W. R. Cheng, G. Wang and Y. Liu, *J Polym Sci Pol Chem*, 2017, **55**, 632-639.
- 34 24. M. Hartlieb, E. G. L. Williams, A. Kuroki, S. Perrier and K. E. S. Locock, *Curr Med Chem*, 2017, **24**,
- 35 2115-2140.
- 36 25. M. M. Konai, B. Bhattacharjee, S. Ghosh and J. Haldar, *Biomacromolecules*, 2018, **19**, 1888-1917.
- 37 26. K. A. Brogden, *Nat Rev Microbiol*, 2005, **3**, 238-250.
- 38 27. H. G. Boman, *Immunological Reviews*, 2000, **173**, 5-16.
- 39 28. I. Sovadinova, E. F. Palermo, M. Urban, P. Mpiga, G. A. Caputo and K. Kuroda, *Polymers*, 2011, **3**, 1512-
- 40 1532.
- 41 29. A. K. Marr, W. J. Gooderham and R. E. W. Hancock, *Current Opinion in Pharmacology*, 2006, **6**, 468-472.
- 42 30. G. N. Tew, R. W. Scott, M. L. Klein and W. F. Degrado, *Accounts Chem Res*, 2010, **43**, 30-39.
- 43 31. A. C. Engler, N. Wiradharma, Z. Y. Ong, D. J. Coady, J. L. Hedrick and Y. Y. Yang, *Nano Today*, 2012, **7**,
- 44 201-222.
- 45 32. H. Takahashi, G. A. Caputo, S. Vemparala and K. Kuroda, *Bioconjugate Chem*, 2017, **28**, 1340-1350.
- 46 33. M. Mizutani, E. F. Palermo, L. M. Thoma, K. Satoh, M. Kamigaito and K. Kuroda, *Biomacromolecules*,
- 47 2012, **13**, 1554-1563.
- 48 34. E. A. Chamsaz, S. Mankoci, H. A. Barton and A. Joy, *ACS Appl Mater Inter*, 2017, **9**, 6704-6711.
- 49 35. V. W. L. Ng, J. P. K. Tan, J. Y. Leong, Z. X. Voo, J. L. Hedrick and Y. Y. Yang, *Macromolecules*, 2014,
- 50 **47**, 1285-1291.
- 51 36. D. N. Amato, D. V. Amato, O. V. Mavrodi, W. B. Martin, S. N. Swilley, K. H. Parsons, D. V. Mavrodi and
- 52 D. L. Patton, *ACS Macro Lett*, 2017, **6**, 171-175.
- 53 37. M. Vert, *Biomacromolecules*, 2005, **6**, 538-546.
- 54 38. A. Sagi, R. Weinstein, N. Karton and D. Shabat, *J Am Chem Soc*, 2008, **130**, 5434+.
- 55 39. S. T. Phillips and A. M. DiLauro, *ACS Macro Lett*, 2014, **3**, 298-304.

- 1 40. G. I. Peterson, M. B. Larsen and A. J. Boydston, *Macromolecules*, 2012, **45**, 7317-7328.
- 2 41. A. D. Wong, M. A. DeWit and E. R. Gillies, *Adv Drug Deliver Rev*, 2012, **64**, 1031-1045.
- 3 42. B. Fan, J. F. Trant, A. D. Wong and E. R. Gillies, *J Am Chem Soc*, 2014, **136**, 10116-10123.
- 4 43. M. Shamis, H. N. Lode and D. Shabat, *J Am Chem Soc*, 2004, **126**, 1726-1731.
- 5 44. H. Wang, Q. Huang, H. Chang, J. R. Xiao and Y. Y. Cheng, *Biomater Sci-Uk*, 2016, **4**, 375-390.
- 6 45. Y. Xie, T. Murray-Stewart, Y. Z. Wang, F. Yua, J. Li, L. J. Marton, R. A. Casero and D. Oupicky, *J Control Release*, 2017, **246**, 110-119.
- 7
- 8 46. A. M. DiLauro, G. G. Lewis and S. T. Phillips, *Angew Chem Int Edit*, 2015, **54**, 6200-6205.
- 9 47. H. Zhang, K. Yeung, J. S. Robbins, R. A. Pavlick, M. Wu, R. Liu, A. Sen and S. T. Phillips, *Angew Chem Int Edit*, 2012, **51**, 2400-2404.
- 10
- 11 48. A. P. Esser-Kahn, S. A. Odom, N. R. Sottos, S. R. White and J. S. Moore, *Macromolecules*, 2011, **44**, 5539-5553.
- 12
- 13 49. M. S. Baker, H. Kim, M. G. Olah, G. G. Lewis and S. T. Phillips, *Green Chem*, 2015, **17**, 4541-4545.
- 14 50. C. Ergene and E. F. Palermo, *Biomacromolecules*, 2017, **18**, 3400-3409.
- 15 51. M. G. Olah, J. S. Robbins, M. S. Baker and S. T. Phillips, *Macromolecules*, 2013, **46**, 5924-5928.
- 16 52. K. Yeung, H. Kim, H. Mohapatra and S. T. Phillips, *J Am Chem Soc*, 2015, **137**, 5324-5327.
- 17 53. K. Hu, N. W. Schmidt, R. Zhu, Y. J. Jiang, G. H. Lai, G. Wei, E. F. Palermo, K. Kuroda, G. C. L. Wong and L. H. Yang, *Macromolecules*, 2013, **46**, 1908-1915.
- 18
- 19 54. X. Yang, K. Hu, G. T. Hu, D. Y. Shi, Y. J. Jiang, L. W. Hui, R. Zhu, Y. T. Xie and L. H. Yang, *Biomacromolecules*, 2014, **15**, 3267-3277.
- 20
- 21 55. S. Chakraborty, R. H. Liu, Z. Hayouka, X. Y. Chen, J. Ehrhardt, Q. Lu, E. Burke, Y. Q. Yan, B. Weisblum, G. C. L. Wong, K. S. Masters and S. H. Gellman, *J Am Chem Soc*, 2014, **136**, 14530-14535.
- 22
- 23 56. M. Alvarez-Paino, A. Munoz-Bonilla, F. Lopez-Fabal, J. L. Gomez-Garces, J. P. A. Heuts and M. Fernandez-Garcia, *Biomacromolecules*, 2015, **16**, 295-303.
- 24
- 25 57. E. H. H. Wong, M. M. Khin, V. Ravikumar, Z. Y. Si, S. A. Rice and M. B. Chan-Park, *Biomacromolecules*, 2016, **17**, 1170-1178.
- 26
- 27 58. S. Colak, C. F. Nelson, K. Nusslein and G. N. Tew, *Biomacromolecules*, 2009, **10**, 353-359.
- 28 59. A. Punia, A. Mancuso, P. Banerjee and N. L. Yang, *ACS Macro Lett*, 2015, **4**, 426-430.
- 29 60. A. Punia, K. Lee, E. He, S. Mukherjee, A. Mancuso, P. Banerjee and N. L. Yang, *Int J Mol Sci*, 2015, **16**, 23867-23880.
- 30
- 31 61. B. C. Allison, B. M. Applegate and J. P. Youngblood, *Biomacromolecules*, 2007, **8**, 2995-2999.
- 32 62. P. H. Sellenet, B. Allison, B. M. Applegate and J. P. Youngblood, *Biomacromolecules*, 2007, **8**, 19-23.
- 33 63. E. F. Palermo and K. Kuroda, *Appl Microbiol Biot*, 2010, **87**, 1605-1615.
- 34 64. H. Takahashi, E. F. Palermo, K. Yasuhara, G. A. Caputo and K. Kuroda, *Macromol Biosci*, 2013, **13**, 1285-1299.
- 35
- 36 65. K. Kuroda and G. A. Caputo, *Wires Nanomed Nanobi*, 2013, **5**, 49-66.
- 37 66. M. V. Kameneva, J. F. Antaki, K. K. Yeleswarapu, M. J. Watach, B. P. Griffith and H. S. Borovetz, *Asaio Journal*, 1997, **43**, M571-M575.
- 38
- 39 67. M. V. Kameneva, B. M. Repko, E. F. Krasik, B. C. Perricelli and H. S. Borovetz, *Asaio Journal*, 2003, **49**, 537-542.
- 40
- 41 68. K. Lienkamp, A. E. Madkour, A. Musante, C. F. Nelson, K. Nuesslein and G. N. Tew, *J Am Chem Soc*, 2008, **130**, 9836-9843.
- 42
- 43 69. K. Lienkamp, K. N. Kumar, A. Som, K. Nusslein and G. N. Tew, *Chem-Eur J*, 2009, **15**, 11710-11714.
- 44 70. K. Kuroda, G. A. Caputo and W. F. DeGrado, *Chem-Eur J*, 2009, **15**, 1123-1133.
- 45 71. P. Stiefel, S. Schmidt-Emrich, K. Maniura-Weber and Q. Ren, *Bmc Microbiol*, 2015, **15**.
- 46 72. L. H. Yang, V. D. Gordon, D. R. Trinkle, N. W. Schmidt, M. A. Davis, C. DeVries, A. Som, J. E. Cronan, G. N. Tew and G. C. L. Wong, *P Natl Acad Sci USA*, 2008, **105**, 20595-20600.
- 47
- 48 73. H. Choi, S. Chakraborty, R. H. Liu, S. H. Gellman and J. C. Weisshaar, *ACS Chem Biol*, 2016, **11**, 113-120.
- 49
- 50 74. S. Hovakeemian, R. H. Liu, S. H. Gellman and H. Heerklotz, *Biophys J*, 2015, **108**, 551a-551a.
- 51 75. S. G. Hovakeemian, R. H. Liu, S. H. Gellman and H. Heerklotz, *Soft Matter*, 2015, **11**, 6840-6851.
- 52 76. E. F. Palermo, D.-K. Lee, A. Ramamoorthy and K. Kuroda, *J Phys Chem B*, 2011, **115**, 366-375.
- 53
- 54
- 55